Lasers in Manufacturing Conference 2015

Online Crack Detection During Laser Welding Using Passive Thermography

Daniel Weller*[a], Peter Stritt[a], Florian Fetzer[a], Rudolf Weber[a], Thomas Graf[a]

Cyrille Bezençon[b], Jörg Simon[b], Corrado Bassi[b]

[a]*Institut fuer Strahlwerkzeuge (IFSW), Pfaffenwaldring 43, 70569 Stuttgart, Germany*
[b]*Novelis Switzerland SA, Rte des Laminoirs 15, 3960 Sierre, Switzerland*

Abstract

The non-destructive testing of laser welds within the process chain of industrial production is of prime importance for the quality assurance. In this paper passive thermography was used to detect centerline cracks. These hot cracks are likely to occur when welding car body sheets in an overlap configuration close to the edge. Welding at this position leads to a strong heat accumulation. This results in a non-symmetric temperature field causing a heat flow from the edge into the body across the weld seam. If the weld seam is split due to a centerline crack this heat flow is significantly disturbed. It was found that this characteristic change of the heat flow is clearly measurable and can be utilized to detect hot cracking during welding using an infrared camera.

Keywords: Laser Welding, 6000 Series Aluminum, Hot Cracking, Thermography, Process Monitoring

1. Introduction

Laser welding processes are well established in the automated mass production, such as in the automotive industry. Since the introduction of the remote laser welding technology flexible weld shapes and fast positioning are possible. To guarantee a constant product quality in high volume applications fast, reliable and cost-effectively process monitoring is required.

* Corresponding author. Tel.: +49-711-68564146; fax: +49-711-68554146.
E-mail address: daniel.weller@ifsw.uni-stuttgart.de.

Hot Cracks are one of the important weld defects to monitor in car body production. 6000 series (magnesium and silicon based) aluminum alloys used as a lightweight material are susceptible to hot cracking during laser welding. Centerline hot cracks are forming at the trailing end of the weld pool due to an overload caused by tensile stresses and strains as mentioned by Pellini, 1952. This thermo-mechanical load is due to the shrinkage during solidification and the temperature gradients during welding. The temperature gradients and therefore the hot cracking sensitivity are influenced by the process parameters and the weld position on the work piece as summarized by Cross, 2005. If the weld position on sheets with a thickness of about 2.7 mm is below a distance of 10 mm to the edge the temperature gradient at the trailing end of the weld pool is affected by a reflected heat flow from the edge, shown by Weller, 2013. This affected temperature gradient leads to a changed thermo-mechanical load which is one reason for centerline hot cracks in welds placed at distances between 3 to 6 mm from the edge of the work piece as investigated by Hilbinger, 2000 or Stritt et al., 2012. Welds at these positions are typical for flange joints in car body production.

2. The principle of measurement

In Fig. 1 the temperature field of a crack-free weld (a) and a weld with a centerline crack (b) is shown. These temperature fields were calculated with finite element numerical welding process modelling using the routines from Stritt et al., 2012. The applied heat source is calibrated by weld cross sections gained from experiments done at different edge distances. The simulation is three-dimensional and takes temperature dependence of heat conductivity, heat capacity and density into account. In the modelled temperature fields, shown in Fig. 1, two 6000 series aluminum sheets with thicknesses of 1.2 mm on the top and 1.7 mm on the bottom were processed. The welding process was modelled with a feed rate of 6 m/min, a laser power of 5 kW, a spot diameter of 650 µm and an edge distance of 5 mm.

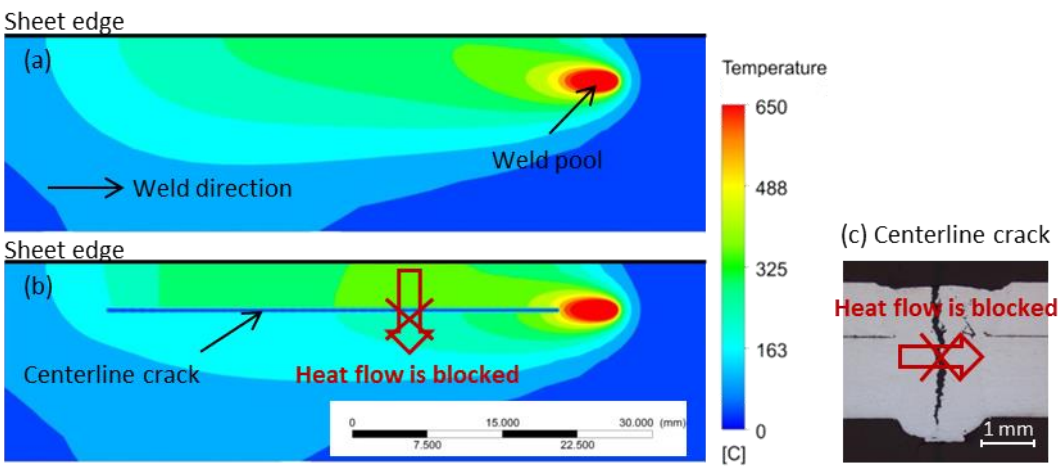

Fig. 1. (a) Temperature field of a crack-free weld calculated with a finite numerical welding process modelling; (b) Calculated temperature field with a centerline crack; (c) Cross-section of an overlap weld from two 6000 series aluminum alloy sheets; Process parameter for (a), (b), (c): P = 5 kW, v = 6 m/min, d_f = 650 µm, edge distance a = 5 mm, sheet thickness s = 1.2 mm (top) and s = 1.7 mm (bottom).

Part (c) of Fig. 1 shows a weld cross section of the corresponding experiment of two welded 6000 series aluminum sheets with a typical centerline crack. As can be seen, this centerline crack splits the weld and therefore prevents the heat from flowing from one side of the crack to the other. To implement the thermal effect of a centerline crack into the modelling the temperature was set to ambient temperature t = 25°C permanently and the heat conduction was set to zero permanently at the position of the crack after each time step.

At the edge of the sheet the heat is reflected resulting in a non-symmetric temperature field as can be seen for both temperature fields shown in Fig. 1. This causes a heat flow from the edge into the body of the welded sheets across the weld seam. If a centerline crack occurs the heat flow across the weld is significantly disturbed. This characteristic change of the temperature field will be used as a principle of measurement for the method of online crack-detection proposed in this paper.

3. Experiments

3.1. Experimental setup

To prove the above introduced principle of crack diagnostics experiments using an infrared camera with a frame rate of 50 Hz to analyze the arising temperature field were made. To reduce the dependence on the local emissivity, the aluminum sheets were coated with a black graphite layer. All experiments were done with a TruDisk 5001 laser and a fiber delivery with a 200 µm core diameter. The laser has a maximum output power of 5000 W at a wavelength of 1030 nm. To focus the laser beam on the work piece a PFO 3D scanner optics with a focal length of 450 mm was used. This yields a focus diameter of 650 µm. No shielding gas was used.

3.2. Multi-alloy aluminum

Beside the thermo-mechanical effects described in chapter 1, the metallurgical properties of materials are related to the hot cracking sensitivity. One reason for the crack initiation when welding 6000 series aluminum alloys is the dendrite-solidification structure. If the residual melt is not able to fill up the volume between the dendrite network in the solidification zone a crack forms by lack of material. Studies by Borland, 1960 and Feurer, 1977 have shown, that increasing the fraction of silicon in a 6000 series aluminum alloy raises the ability to fill up these gaps between the dendrite structures. Furthermore welds with aluminum alloys with a higher silicon fraction result in grain refinement and reduced solidification shrinkage and therefore a lower hot cracking susceptibility as observed by Coniglio et al., 2008.

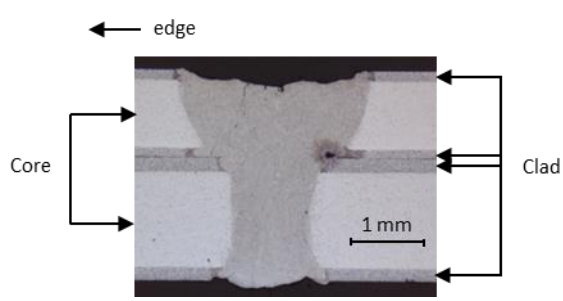

Fig. 2. Cross section of two welded AA6xxx series multi-alloy aluminum sheets. Process parameter: P = 5 kW, v = 6 m/min, d_f = 650 µm, edge distance a = 5 mm

Building upon that concept a common way to avoid hot cracks is the use of silicon-rich filler material investigated by Coniglio et al., 2008.

For the experiments a standard AA6014 aluminum alloy and a multi-alloy aluminum, NF Ac-200RW by Novelis were used. This fusion-bonded multi-alloy aluminum consists of a core material and two outer cladding layers as can be seen in Fig. 2. The core material maintains all the advantages and required properties of an AA6xxx monolithic alloy while the cladding has a high silicon content. During the welding process the layers are mixing and the hot cracking sensitivity is reduced as proven by Bezençon et al., 2011. This multi-alloy aluminum is designed for the remote laser welding technology because it makes an additional filler wire for the welding process obsolete.

Using the multi-alloy and the monolithic aluminum alloy as materials for the experiments, enables a crack-free and cracked weld seam at the same critical edge distance a = 5 mm which is required to compare the arising temperature fields under equal conditions.

3.3. Experimental results

Fig. 3 shows measured temperature distributions in false colors based on the intensity measured by the infrared camera. The color bar goes from blue (cold) to red (hot).

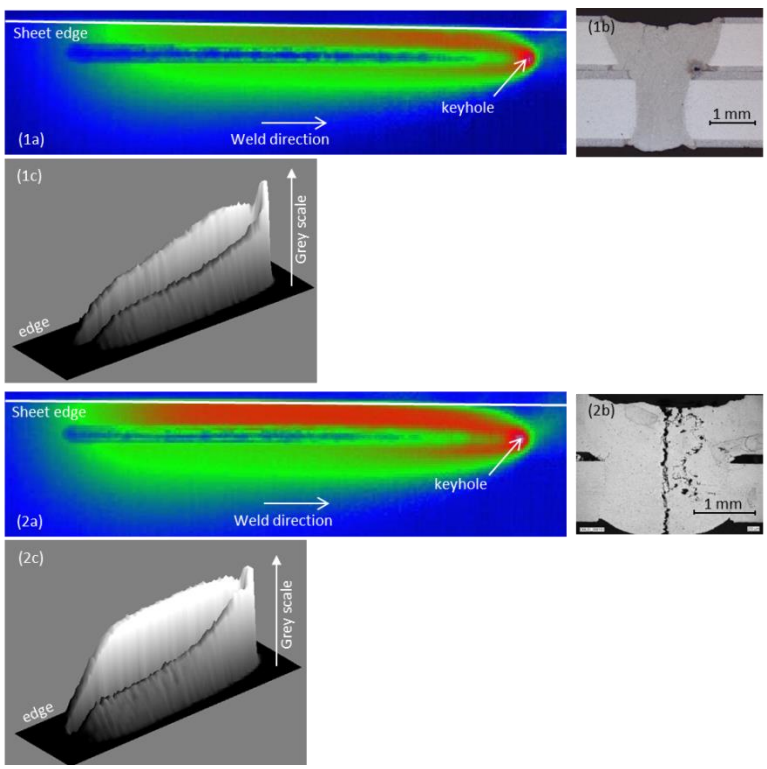

Fig. 3. Comparison of welds without (1) and with (2) cracks: (1a) single frame of infrared video in false colors; (1b) cross section of welded sheets. (1c) surface plot of grey values from infrared video; (2a) single frame of infrared video in false colors; (2b) cross section of welded sheets; (2c) surface plot of grey values from infrared video; Process parameter for (1), (2): P = 5 kW, v = 6 m/min, d_f = 650 µm, edge distance a = 5 mm.

Fig. 3 (1a) shows a frame of the infrared video at the end of the welding process for the crack-free weld with multi-alloy aluminum. Fig. 3 (2a) shows the weld with a centerline crack for the standard monolithic aluminum. Due to the destroyed graphite layer in the weld seam, the emissivity is decreased there and the temperature appears lower in that region, even though this is actually not the case.

Comparing the frames (1a) and (2a) in Fig. 3 with the simulated temperature fields in Fig. 1 shows a good qualitative agreement of the experiment with the expected temperature distribution by the numerical welding process modelling. For the frame (2a) with centerline crack the dark red area on the edge side is larger compared to the frame (1a) from the video of the non-cracked weld. The surface plots (1c) and (2c) generated from these frames confirm this conclusion. The surface plot (2c) with the centerline crack shows a constant high temperature level on the edge side whereas the surface plot (1c) for the non-cracked sample shows a temperature decrease from front to the end of the weld. Therefore the difference of the temperature fields is clearly measurable and can be utilized to detect centerline cracks at close-edge welding.

4. Utilization of temperature signal to detect hot cracking at close-edge welding

To utilize the measured temperature signal to detect hot cracking during welding a certain criterion has to be defined to decide whether there is a centerline crack detected or not. Two different possible approaches will be presented.

4.1. Monitoring the temperature at two positions fixed in space

Fig. 4 (a) shows the position of the measuring point on the edge side and the measuring point on the body side in the infrared video from the experiments. The measuring points were at the fixed position shown in Fig. 4 (a).

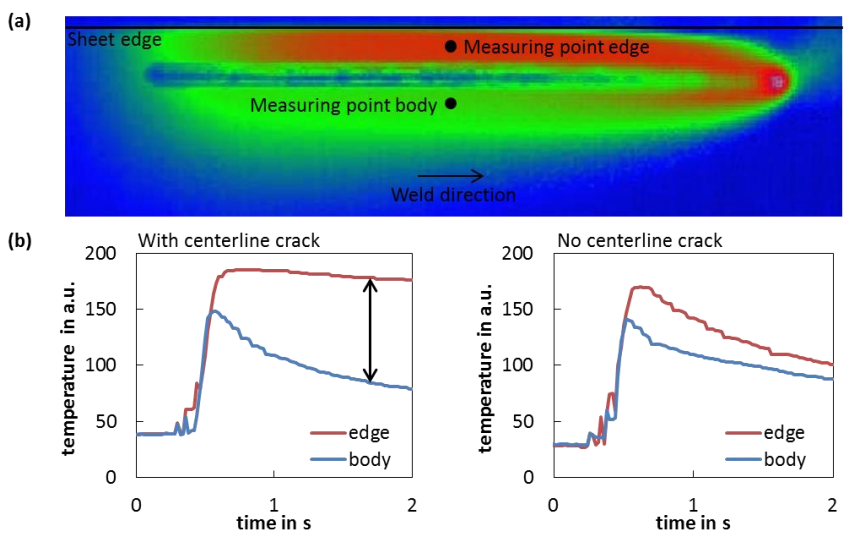

Fig. 4. (a) Frame of infrared video in false colors of the weld with a centerline crack, P = 5 kW, v = 6 m/min, d_f = 650 µm, edge distance a = 5 mm, AA6014 aluminum alloy; (b) The temperature in arbitrary units over time curves of the infrared videos for a measure point on the edge side and on the body side for both cases the cracked and non-cracked weld.

The temperature at these positions is plotted as a function of time for the complete weld in Fig. 4 (b) for both cases cracked (left) and non-cracked (right). At t = 0.5 s the laser beam passes the measuring points and a strong increase of the temperature occurs. On the edge side (red line) the temperature rises higher compared to the temperature on the body side (blue line) due to the reflected heat on the edge.

After the pass by of the laser beam the cooling phase starts immediately. Comparing the two charts in Fig. 4 (b) shows a characteristic difference of the cooling curves. If there is no centerline crack the cooling behavior of both measuring points look very similar whereas with a centerline crack the cooling rate of the measuring point at the edge is obvious slower (red curve left). When the measuring points are positioned in the middle of the weld length as shown in Fig. 4 (b) the slope of the cooling curve on the edge side was found to be lowest. Therefore this position is best to detect a centerline crack due to the big difference in temperature curves. Monitoring the temperature at two spatially fixed positions can be utilized very simple with two pyrometers.

4.2. Monitoring the temperature in line with the welding process

Applying the introduced principle of crack detection on moving optics the temperature was measured in line with the welding process. The temperature field was measured applying a moving coordinate system according to the movement of the laser beam. Thereby three different phases occur during welding, the starting phase, the steady state and the cooling phase. During the steady state the heat input is equal to the heat loss which results in a steady temperature field. At the beginning of the weld and in the cooling phase after the welding process the heat flow is varying yielding a varying temperature field.

In Fig. 5 temperature line plots along the black lines which are orthogonal to the weld of the calculated temperature field in the steady state of the welding process are shown. The temperature curves compare both cases, the cracked weld (red line) and the non-cracked weld (blue line).

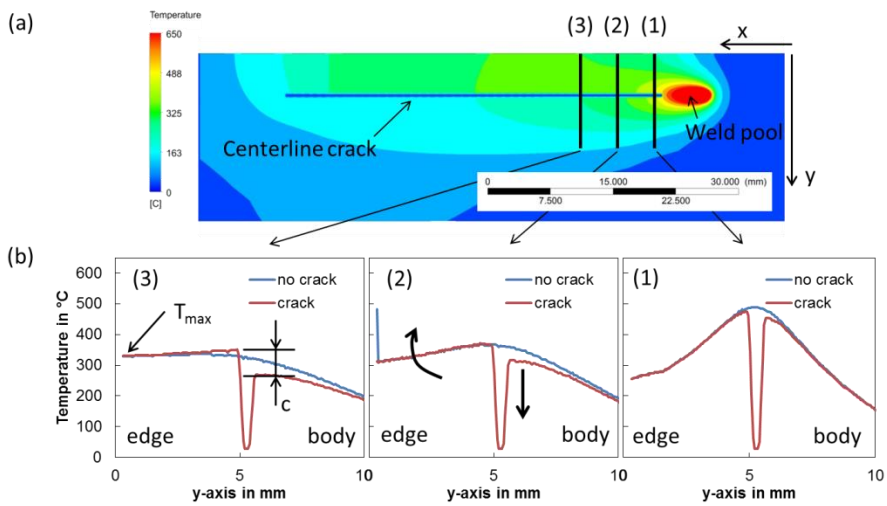

Fig. 5. Transverse temperature line plots (b) along the black lines of the calculated temperature field (a) in the steady state of the welding process. Process parameter: P = 5 kW, v = 6 m/min, d_f = 650 µm, edge distance a = 5 mm, sheet thickness s = 1.2 mm (top) and s = 1.7 mm (bottom).

The position of line plot (1) is at the trailing end of the weld pool where the centerline crack originates. Except of the dip in the cracked temperature curve due to a point of discontinuity (described in section 2) the two temperature signals are identical. Meaning there is no differentiation recognizable and therefore no crack detection possible. At position (2) the heat flow of the line plot with the centerline crack is already blocked and a temperature step at the position of the crack (dip in red curve) from the edge side to the body side is noticeable. On the body side the temperature drops due to a lack of heat flow from the edge side. On the edge side the temperature is rising for both cases due to the reflected heat on the edge. Shifting the transverse line further to position (3) the heat accumulation increases and the temperature on the edge is higher compared to the position at the center of the weld for the non-cracked case (blue line). At position (3) the temperature step, marked with the symbol *c*, is higher compared to position (2). The higher this temperature step, the better it can be detected and used as detection criterion for centerline hot cracks.

Fig. 6 (a) shows the temperature fields calculated at three different points in time for the condition with centerline crack. The distance of the temperature measuring line (vertical black line) to the weld pool corresponds to position (3) in Fig. 5. Fig. 6 (b) depicts the temperature curve at t = 0.3 s measured along the black line shown in Fig. 6 (a). Again the temperature step at the centerline crack from the edge to the body side is observable. To monitor the behavior of the height of the temperature step during the welding process two measuring points, T_{edge} and T_{body}, were set as shown in Fig. 6 (b). Fig. 6 (c) shows the temperature curves of these two points over time with the three phases during the welding process. In the cooling phase the two points stay at the last position of the weld process.

In the beginning of the welding process no crack occurs and the temperature of the two monitored points are identical. At t = 0.16 s (1) the centerline crack starts to form as was seen in the experiment. Still no difference between the two temperatures at the measuring points can be seen because they have not reached the crack yet. At t = 0.2 s (2) the monitored points have the x-coordinate of the beginning of the crack. From this point in time the heat flow from the edge to the body side is blocked.

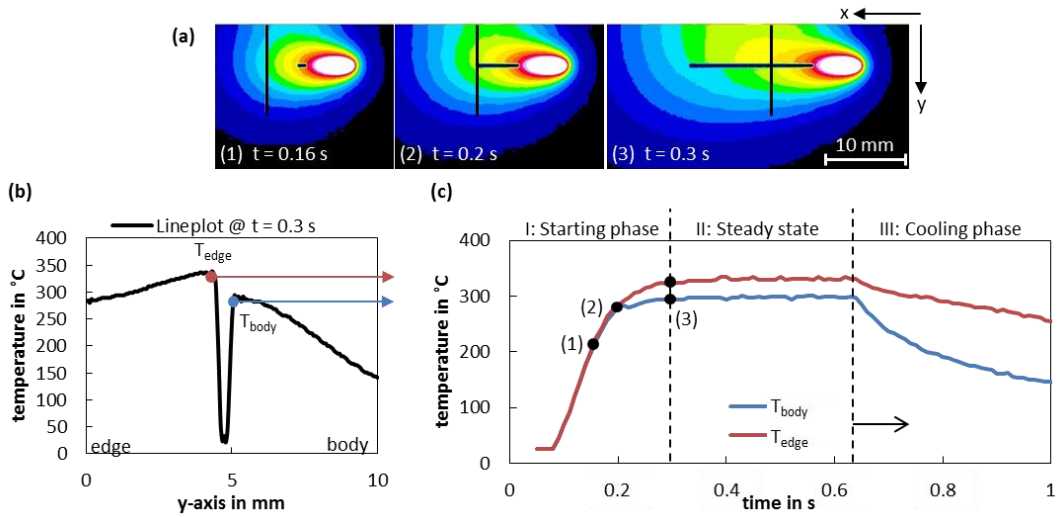

Fig. 6. (a) Simulated temperature field at three different points in time; (b) Transverse line plot of temperature curve at t = 0.3 s; (c) Temperature step at position of centerline crack over time. Process parameter: P = 5 kW, v = 6 m/min, d_f = 650 µm, edge distance a = 5 mm, sheet thickness s = 1.2 mm (top) and s = 1.7 mm (bottom).

The temperature on the body side stays constant whereas the temperature on the edge rises further. At t = 0.3 s the steady state is reached and therefore the maximum temperature step at the monitored position. After completion of the welding process the cooling rate on the edge side (red line) is lower compared to the body side (blue line). This enhances the temperature step at the centerline crack between the body side and the edge side.

5. Conclusion

The investigations of the temperature field during welding show that welding close to the edge leads to heat accumulation which results in heat flow into the body. A centerline crack occurring during welding is changing this heat flow and with it the temperature field significantly. It was found that this characteristic change can be used as a principle for online crack-detection. To utilize this principle two methods were discussed.

First, when monitoring the temperature at two spatially fix positions the behavior of the cooling rate can be analyzed. If a centerline crack occurs during welding, this can be detected by a significant lower slope for the cooling curve on the edge side compared to the body side. This principle can be utilized very easily measuring the temperatures at these two positions with two pyrometers. However, it is not simply practicable for remote welding applications with moving optics.

Second, to utilize the principle of measurement for moving optics the temperature signal was monitored at a fixed position behind the welding pool. In that case the characteristic feature to detect a weld with a centerline crack is a significant temperature step when monitoring the temperature across the weld from the edge into the body. The level of this temperature step is dependent on the monitoring position. Shifting this position away from the weld pool enhances the level of the temperature step. Yet, this will delay the time of first detection by the monitor system. Monitoring the temperature at a fixed position behind the weld pool enables a crack detection on-the-fly during the welding process using remote technology.

References

Bezençon, C., André, P.-D., Bassi, C., 2011, Remote Laser Welding of AA6xxx Multi-Layer Fusion™ Material, in proceedings of LATEST2 Joining Conference.

Borland, J.C., 1960, Generalized theory of super-solidus cracking in welds (and castings), British Welding Journal 7, 508-512.

Coniglio, N., Cross, C. E., Michael, T., Lammers, M., 2008, Defining a Critical Weld Dilution to Avoid Solidification Cracking in Aluminum, Welding Journal, Vol. 87.

Cross, C.E., 2005, On the Origin of Weld Solidification, Hot Cracking Phenomena in Welds I, pp 3-18, Springer Berlin Heidelberg.

Feurer, U., 1977, Influence of alloy composition and solidification conditions on dendrite arm spacing, feeding and hot tearing properties of aluminium alloys, Proceedings International Symposium on Engineering Alloys, 131-145

Hilbinger, R.M., 2000, Heissrissbildung beim Schweißen von Aluminium in Blechrandlage, Dissertation Bayreuth, Herbert Utz Verlag.

Pellini, W. S. 1952. Strain theory for hot tearing. Foundry 80: 125–199.

Stritt, P., Weber, R., Graf, T., Mueller, S., Weberpals, J.-P., 2012, New hot cracking criterion for laser welding in close-edge position, in Proceedings of ICALEO.

Weller, D., Bezençon, C., Stritt, P., Weber, R., Graf, T., 2013, Remote Laser Welding of Multi-alloy Aluminum at Close-edge Position, in Physics Procedia, volume 41, pages 164-168.